NEOPLASIA
www.neoplasia.com

Volume 27 Number xxx Month 2022 pp. 100780

Article

Influence of alectinib and crizotinib on ionizing radiation - *in vitro* analysis of ALK/ROS1-wildtype lung tissue cells

Tina Jost[a,b,*]; Ann-Kristin Schultz[a]; Benjamin Frey[a,b,c]; Jennifer Vu[a]; Rainer Fietkau[a,b]; Luitpold V. Distel[a,b,1]; Markus Hecht[a,b,1]

[a] Department of Radiation Oncology, University Hospital Erlangen, Friedrich-Alexander-Universität Erlangen-Nürnberg, Erlangen 91054, Germany
[b] Comprehensive Cancer Center Erlangen-EMN (CCC ER-EMN), Erlangen 91054, Germany
[c] Deutsches Zentrum Immuntherapie, Erlangen, Germany

Abstract

(1) Background: Just little is known about the interaction of ALK/ROS1-targeting kinase inhibitors with ionizing radiation (IR), particularly regarding side effects. We investigated the toxicity in two different lung cell lines both ALK/ROS1 wildtype (healthy and tumor origin) as representatives for normal lung tissue; (2) Methods: Human lung cell line BEAS-2B and malignant A549 lung cancer cells (ALK/ROS1 wt) were treated with alectinib or crizotinib, 2 Gy irradiation or a combination of KI and IR. Cell toxicity was analyzed by cell death (Annexin, 7AAD), colony forming, migration assay and live-cell imaging (TMRM, DRAQ7, Caspase3/7). Cell cycle (Hoechst) were analyzed by flow cytometry; (3) Results: Crizotinib led to higher cell death rates than alectinib, when cells were treated with 10 µM KI. Alectinib induced a more intense growth inhibition of colonies. Both inhibitors showed additive effects in combination with irradiation. Combination treatment (IR + KI) does not lead to synergistic effect on neither cell death nor colony forming; (4) Conclusions: The influence of simultaneous KI and IR was studied in non-mutated ALK/ROS1 cell lines. Both KIs seems to be well tolerated in combination with thoracic radiotherapy and lacked synergistic reinforcement in cellular toxicity. This supports the feasibility of ALK/ROS1 inhibition in combination with thoracic irradiation in future clinical trials.

Neoplasia (2022) 27, 100780

Keywords: Lung cells, Alectinib, Crizotinib, Radiotherapy, Normal tissue, Side effects

Introduction

With more than 300.000 cases in EU-27 in 2020 lung cancer is still the second most-common malignancy in male and third most-common in female (ECIS). Different biomarkers are established for the selection of precise systemic therapy of metastatic non-small cell lung cancer (NSCLC). Relevant mutations like epidermal growth factor receptor (EGFR) mutations, anaplastic lymphoma kinase (ALK) rearrangements, ROS1 rearrangements, and BRAF V600E mutations are molecularly tested and approximately 30 % of NSCLC patients harbor one or more of these alterations [1].

First-generation kinase inhibitor crizotinib was approved by the EMA in 2012 for monotherapy (first-line) in ALK-positive and/or ROS1-positive NSCLC. Beside ALK and ROS, crizotinib targets multiple proteins like hepatocyte growth factor receptor (HGFR, c-Met), and récepteur d'origine nantais (RON) additionally (FDA Approval; Reference ID: 4730020). Second-generation KI alectinib, approved in 2017 by the EMA as first-line monotherapy or second-line after crizotinib in ALK-positive NSCLC, blocks the STAT3 and PI3K/ACT pathways and therefore lead to cell death, by inhibiting the tyrosine kinases ALK and RET (FDA Approval; Reference ID: 4177381). Alectinib overcomes the blood-brain-barrier and leads to a reduction of progression in the central nervous system (CNS) significantly (Alectinib 12 % versus crizotinib 45 %) [2].

In the metastatic situation frequently also, palliative radiotherapy of e.g. brain or bone metastases is required [3–5]. Therefore, the need arises to

* Corresponding author at: Department of Radiation Oncology, University Hospital Erlangen, Friedrich-Alexander-Universität Erlangen-Nürnberg, 91054 Erlangen, Germany
E-mail addresses: tina.jost@uk-erlangen.de (T. Jost), ann-kristinschultz@gmx.de (A.-K. Schultz), Benjamin.frey@uk-erlangen.de (B. Frey), Jennifer.vu@gmx.de (J. Vu), rainer.fietkau@uk-erlangen.de (R. Fietkau), Luitpold.distel@uk-erlangen.de (L.V. Distel), markus.hecht@uk-erlangen.de (M. Hecht).
[1] These authors contributed equally to this work.
Received 15 October 2021; received in revised form 6 February 2022; accepted 18 February 2022

https://doi.org/10.1016/j.neo.2022.100780

investigate whether the combination of targeted therapy (kinase inhibitors) and ionizing radiation (IR) interact with each other and what type of outcome should be expected, both in the tumor and in the surrounding normal tissue. There is evidence that KI interact with IR especially for inhibitors of BRaf like vemurafenib and dabrafenib [6]. Severe acute and late toxicities occurred in the past and pausing of the KI during IR is recommended for some small molecules [7,8]. One of the most challenging toxicities in the lung is radiation-related pneumonitis (RP), which is known as acute lung tissue inflammation. Several combinatory treatment settings a published to increase risk of RP. Synergistic interactions of IR and chemotherapy [9] and additionally the combination of IR with inhibitors of EGFR (erlotinib, gefitinib, osimertinib), which are frequently used in NSCLC, were found [10].

Just little is known about the interaction of ALK/ROS1-targeting kinase inhibitors with IR, particularly regarding the occurrence of side effects of the surrounding healthy lung cells. In our study we investigated the toxicity in two different lung cell lines, both ALK and ROS1 wildtype as representatives for the normal lung tissue, including cell death and colony forming ability, covering different ways of action e.g. senescence. These outcomes are of certain interest regarding analysis of early and late toxicities. Both representing different processes in inflammation, the main cause for e.g. RP. Different forms of cell death as well as acute or persistent cell arrest embrace important immunogenic potential through activation and modulation of the immune system [11–13]. Since the cell cycle phases are relevant for radiosensitivity we checked for the distribution of cells during treatment and analyzed the influence on migration behavior, regarding the approval in the metastatic situation. As special outcome we established a live-cell imaging system to detect mitochondrial activity, apoptosis and necrosis over a time period of up to 72 h. Mitochondrial activity is especially interesting, since loss of organization and dysfunction is published in association with lung disease including cancer [14,15]. Our findings should help to better understand the interactions and possible toxicities of concomitant kinase inhibitor and radiotherapy in normal ALK/ROS1 wildtype lung cells.

Materials and methods

Cell lines and kinase inhibitor

As previously published, normal human bronchial epithelium cells (BEAS-2B) were provided by the United Kingdom Sigma/Public Health Consortium [16]. Infection of this epithelial-like growing cell line with adenovirus type 12 (Ad12) and Simian virus 40 (SV40) hybrid virus has led to immortality required for cell culture potential [17,18]. A549 were purchased by CLS cell lines service (Eppelheim, Germany). For continuous cell culture, cells were cultured in Dulbeco's MEM (Gibco, Waltham, MA, USA), including 10 % FBS (Gibco, Waltham, MA, USA) and 1 % penicillin/streptomycin (Gibco, Waltham, MA, USA). All cells were incubated at 37°C in a humidified 5 % CO2 atmosphere. Cells were cultured 50 passages maximum. Kinase inhibitors alectinib (MW 482.62 g/mol) and crizotinib (450.34 g/mol) (both: Selleck Chemicals LLC, Huston, USA) were prepared as stock solution in DMSO (Roth, Karlsruhe, Germany) and stored at – 80°C with a concentration of 1 mM. Required aliquots were thawed freshly prior to each experiment.

Cell death analysis – FACS

Adequate count of cells was seeded into T25-flasks to reach a confluence of around 50 % and settled down over night. On the next day medium was exchanged with cell culture medium containing a reduced amount of 2 % FBS to avoid bias in outcome because of cells triggered strongly for proliferation. Additionally, kinase inhibitor was added in a certain concentration and after 3 h of incubation cells were irradiated with a dose of 2 Gy by an ISOVOLT Titan X-ray generator (GE, Ahrensburg, Germany). After 48 h of incubation cells and supernatant were collected and stained using Annexin-V-APC and 7-AAD (both: BD Biosciences, Franklin Lakes, NJ, USA) for 30 min on ice. Cells were analyzed using a Beckman coulter cytometer (Cytoflex, Beckman Coulter, Brea, CA, USA). Cells neither positive for Annexin-V nor 7-AAD were defined as "alive", Annexin-V-positive and 7-AAD-negativ cells as "apoptotic" and double-positive cells as "necrotic. For data evaluation, the Kaluza analysis software (Beckman Coulter, Brea, CA, USA) was used.

Cell cycle analysis – FACS

Seeding, treatment and incubation of cells were performed according to our cell death assay mentioned above. Cells and supernatant were harvested 48 h after incubation and fixed with 70 % ethanol for 24 h in minimum. Afterwards cells were stained with DNA dye Hoechst 33258 (Molecular Probes, Eugene, OR, USA) for 1 h on ice and analyzed with the Beckman coulter cytometer.

Colony forming assay

Cells were seeded into 6-well-plates and incubated overnight. After settlement cells were treated with kinase inhibitor (alectinib, crizotinib), irradiation (0, 2 or 4 Gy) or a combination of both and incubated for additional 24 h. Medium was exchanged one day after and substituted with standardly used cell culture medium. Plates were incubated 10 to 14 days to form colonies. Afterwards cells were stained with methylene blue (#66725, Sigma Aldrich, München, Germany) for 30 min and colonies were counted consisting of more than 50 cells. Plating efficiency (PE) and survival fraction (SF) were calculated.

Migration analysis – Scratch assay (collective migration)

For investigation of the migration behavior scratch assays were performed. Therefore, 48-well-plates were seeded with cells to reach confluence within 24 h. Cells were starved using 2 %-FBS containing medium for another 24 h in the incubator. After starvation cell monolayer was scratched with a 10 µL pipet tip and medium was securely exchanged with again 2 %-FBS containing medium including relevant concentrations of kinase inhibitors. Additionally, one half of plates was irradiated with a 2 Gy dose. Images were taken at timepoint 0 h immediately after treatment (kinase inhibitor or irradiation) and repeated after 24 h and 48 h. The decreasing area of the scratch was measured and calculated using the image software Biomas (Version V3.07/2012, MSAB, Erlangen, Germany). Overall migration behavior from 0 h to 48 h was analyzed by calculating area under the curve (AUC) from 0 h to 24 h and 24 h to 48 h, leading to a maximum value of "2" synonymous with "no scratch-closing".

RAD51-staining for analysis of HR-status

To analyze if cells are able to use homologous recombination (HR) in an efficient manner we seeded cells onto glass slides until a confluence of 80 % was reached [19,20]. Cells were than treated with 5 µM DNA-PK inhibitor CC-115 (Selleckchem, Houston, TX, USA) for 24 h to block the non-homologous end-joining pathway and force the cells into HR. After incubation glass slides were irradiated with a dose of 10 Gy by an ISOVOLT Titan X-ray generator and 4 h after irradiation cells were fixed with formaldehyde (4 % v/v) and blocked with a 1 % BSA containing solution. Foci of γH2AX and RAD51 were stained with primary mouse antibody anti-γ H2AX (1:1500, Merck, Darmstadt, Germany) and rabbit anti-RAD51 (1:250, abcam, Cambridge, UK). For detection secondary

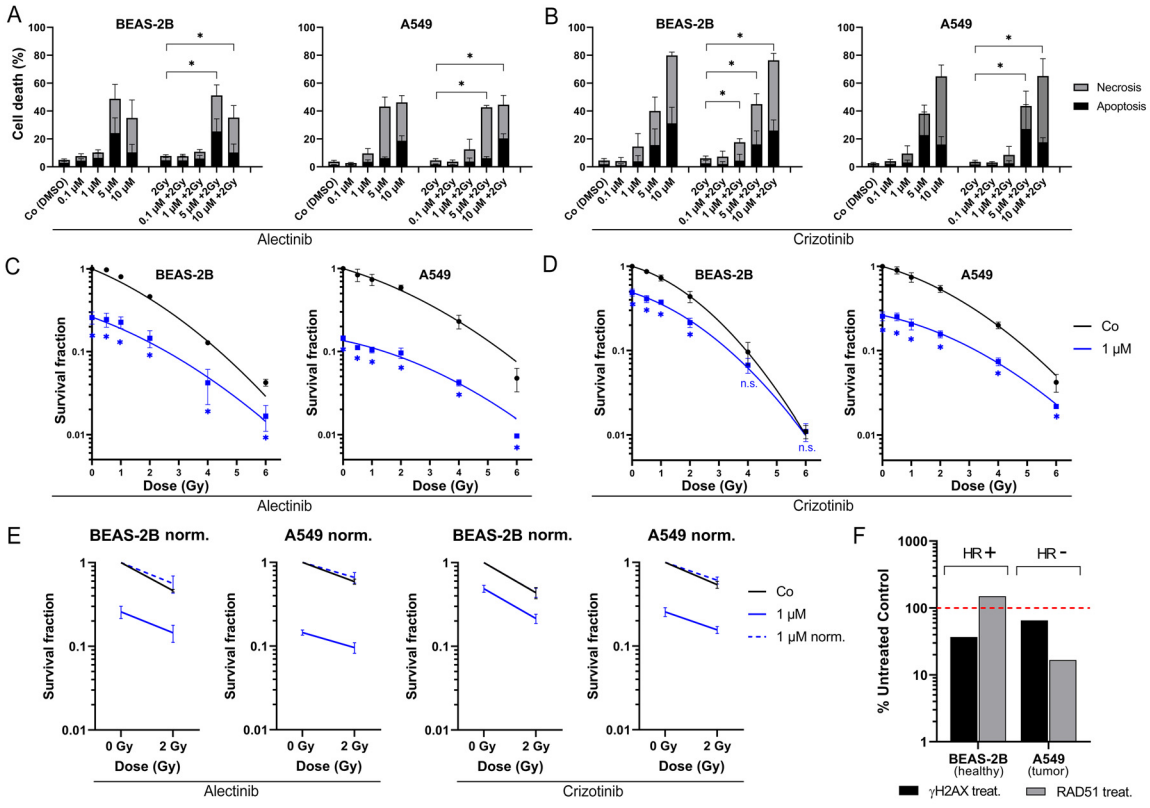

Fig. 1. Cell death analysis and colony forming of ALK/ROS1-wt BEAS-2B and A549 lung cells. Cells were treated with (a) alectinib or (b) crizotinib, 2 Gy irradiation or a combination of KI + IR. Cells died dose-dependent and showed higher cell death rates after crizotinib, unaffected by irradiation ($p < 0.050$). Additionally, relative number of colonies was measured after (c) alectinib and (d) crizotinib (non-linear curve fit). Cells died irradiation- and kinase inhibitor-dependent ($p < 0.050$; one-tailed Mann-Whitney-U). (e) Normalization of colony forming data showed additive effects of the combinatory treatment. (f) Homologous recombination status: staining of γH2AX and RAD51 foci of untreated controls and CC-115 treated (DNA-PK inhibitor) cells. Each value represents mean ± SD (n = 4). Significance was determined by two-tailed Mann Whitney U test * $p \leq 0.050$.

antibodies AlexaFluor488 goat anti-mouse and AlexaFluor594 chicken anti-rabbit (Invitrogen, Eugene, OR, USA) were used. DAPI was applied for DNA staining (10236276001, Sigma Aldrich, St. Louis, MO, USA). Images were taken by a Zeiss Imager Z2 fluorescence microscope (Zeiss, Oberkochen, Germany) and number of foci was automatically counted by Biomas software (Version V3.07/2012, MSAB, Erlangen, Germany) in minimum of 300 cells per condition.

Analysis of mitochondrial activity, apoptosis and necrosis via live-cell imaging

Cells were seeded into T25 flasks. The calculated number of required cells (800,000 cells/mL) correlated with approximately 80 % coverage of the flask's surface. After reaching the adequate cell number, the medium was reduced to 10 mL and the cells were incubated for 45 min with 25 nM Tetramethylrhodamine (TMRM, Invitrogen, Carlsbad, CA, USA) at 37°C and 5 % CO_2. Subsequently, the medium was changed to FluoroBrite^{TM} DMEM (Life Technologies Europe BV, Bleiswijk, Netherlands) and the fluorescent stains DRAQ7 (Abcam, Cambridge, UK) and CellEvent Caspase 3/7 (Invitrogen, Carlsbad, CA, USA) were added with the concentration of 3 μM and 10 μM. Furthermore, 10 mM of Good's Buffer HEPES (Gibco, Waltham, MA, USA) was added. The mixture of cell and stain was parted. After adding 1 μM tyrosinkinase inhibitor (Selleckchem, Houston, TX, USA) to one part, the mixture was divided onto two Rhombic Chamber microfluidic chips (microfluidic ChipShop, Jena, Germany) which were then inserted under the microscope. After 3 h one of the chips was irradiated with 2 Gy by an ISOVOLT Titan X-ray generator (GE, Ahrensburg, Germany). A Leica DM6000B (Leica Microsystems GmbH, Wetzlar, Germany) recorded the images every 20 or 45 min for 3 days with differing wavelengths per each staining. For live cell imaging, the microscope was transformed into an incubating system. Four different positions were attributed to every condition 30–50 individual cells were analyzed within one position. Each experiment was repeated at least 3 times. The imaging analyses was performed with Biomas Software (MSAB, Erlangen, Germany), where the background noise was then reduced, thus allowing the fluorescent color to intensify. The intensities of the different stains were transferred to spreadsheets (Excel, Microsoft Corporation, Redmond, WA, USA) and GraphPad Prism9 (GraphPad Software, San Diego, CA, USA) was then used for data evaluation. Data were normalized to foldchange at $t_0 = 1$.

Statistical analysis

GraphPad prism 9 software (San Diego, CA, USA) was used to perform statistical analysis. Mann-Whitney-U test was used to analyze data. P-value ≤ 0.050 was determined as significant. Graphs were also generated using GraphPad Prism 9 software.

Results

In the following study we investigated the influence of simultaneous kinase inhibitor therapy and ionizing radiation on normal lung tissue

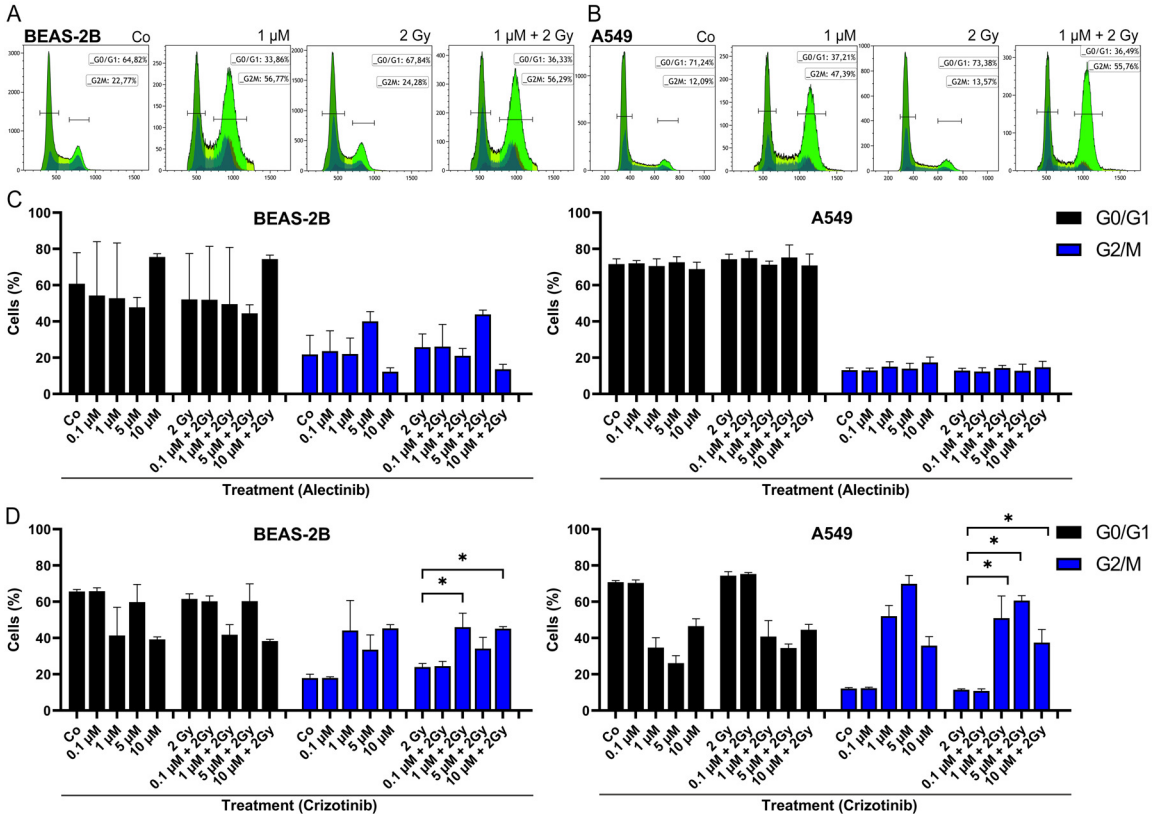

Fig. 2. Cell cycle analysis of BEAS-2B and A549 after mono or combination therapy. Representative histograms and gating strategy after crizotinib w/o 2 Gy IR treatment (a) in BEAS-2B cells and (b) A549 cells. Cells counted in G0/G1 or G2/M phase after treatment with (c) alectinib w/o IR or (d) crizotinib w/o IR. Crizotinib increased number of BEAS-2B cells in G2/M phase after 1 µM + 2 Gy and 10 µM + 2 Gy ($p < 0.050$) and number of A549 cells after 1 / 5 / 10 µM + 2 Gy treatment compared to 2 Gy, respectively. Each value represents mean ± SD (n = 4). Significance was determined by two-tailed Mann Whitney U test * $p \leq 0.050$.

(ALK/ROS1 wt). The first and second generation ALK/ROS1 kinase inhibitors crizotinib and alectinib are approved for treatment of lung malignancies. Since normal tissue is always involved in radiotherapy (surrounding the tumor tissue) we focused on the effect on normal lung cells, based on the absence of ALK/ROS1 mutations, regarding possible side effects previously published for other KI like BRaf-targeting vemurafenib [6]. Cell death and colony formation were measured after combinatory therapy (IR+KI), as well as after monotherapy of kinase inhibitor or irradiation (Fig. 1). Regarding our clinical context of radiation oncology, we always compared our findings between the treatment schemes of 2 Gy vs. combination therapy (IR+KI) [20–22].

KI-dependent cellular toxicity in lung cells

In our cell death analysis, irradiation itself or concomitant with the KI therapy did not lead to enhanced cell death rates and both normal lung cell lines responded equally when treated with the same kinase inhibitor. Nonetheless, we found significant dose-dependent toxicity (apoptosis and necrosis) in both cell lines and after treatment with both inhibitors alectinib (Fig. 1A) and crizotinib (Fig. 1B) ($p < 0.050$). In general, both inhibitors lead to equal rates of cell death at modest concentrations of 0.1 / 1 / 5 µM. Crizotinib resulted in a stronger response at highest concentration of 10 µM in BEAS-2B (10 µM + 2 Gy: 76.4 %) and A549 (10 µM + 2 Gy: 65.2 %) compared to alectinib (BEAS-2B, 10 µM + 2 Gy: 35.3 %; A549, 10 µM + 2 Gy: 44.5 %).

As a special approach, a live-cell microscope was used for time-resolved development of mitochondrial activity, apoptosis and necrosis. A549 and BEAS-2B cells (ALK/ROS1 wt) were treated as mentioned above with alectinib or crizotinib in addition to IR (Co, 1 µM, 2 Gy, 1 µM + 2 Gy), stained and images were acquired every 20 or 45 min, respectively. Data of the intensity of the fluorescence was accumulated as described in the material and methods section to generate curves over time for cell line A549 (Fig. S1A) and BEAS-2B (Fig. S1B). All treatment arms showed similar outcome in most cases. Just BEAS-2B cells responded with a slight increase of apoptosis and necrosis approximately 36 h after 2 Gy IR or combination therapy (IR + KI) (Supplementary Figs. S1 and S3).

Combination treatment (IR + KI) does not lead to synergistic decline of colony forming

Since staining of apoptosis and necrosis gives insights in cellular processes of cell death, we additionally used the gold standard in radiation biology to cover a wider range of cellular processes like cell survival, clonogenicity and senescence (Fig. 1C–E). After treatment with 1 µM KI, which represents a more physiological relevant concentration (Alecensa; FDA approval "prescribing information"), colony formation decreased in a radiation dose-dependent manner in both cell lines. Alectinib showed a stronger reduction of colonies (BEAS-2B: 25 %, A549: 14 %) compared to crizotinib (BEAS-2B: 48 %, A549: 25 %). Clonogenicity was stronger reduced in A549 cells than in BEAS-2B cells, especially after treatment with crizotinib. Most importantly, normalized data (dashed, blue lines) of BEAS-2B and A549 gave evidence that

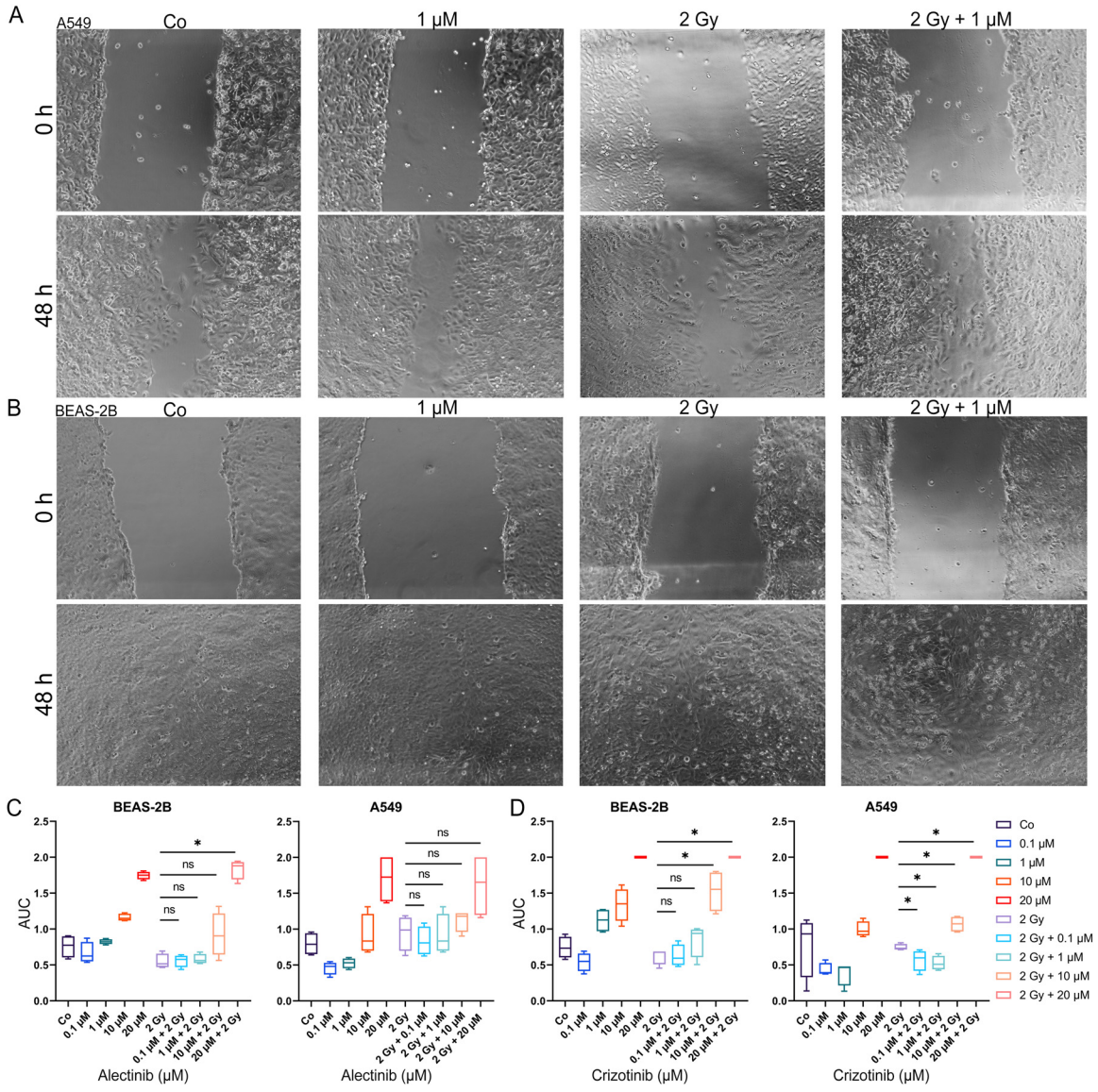

Fig. 3. Influence of ALK/ROS1 inhibitors alectinib and crizotinib on migration behavior of ALK/ROS1-wt cell lines. Representative microscopic images of scratch closing at timepoints 0 h and 48 h under alectinib w/o 2 Gy IR of A549 (a) and BEAS-2B (b). BEAS-2B and A549 cells were treated with alectinib (c) or crizotinib (d) for 48 h and decrease of scratch area was measured. AUC of the time-lapse data was calculated to compare different treatment regimens (maximum of "2" represents no migration). Boxplots of AUC data for complete dose-escalation (0.1 – 20 µM KI) of both inhibitors alectinib and crizotinib, 2 Gy irradiation and the combinatory treatment regime. Each value represents median (min to max) (n = 4). Significance was determined by two-tailed Mann Whitney U test * $p \leq 0.050$.

these KI influence irradiation in an additive, primary IR-depended manner (Fig. 1E), but not synergistically.

To handle DNA damage after irradiation, cells need adequate efficiency of several DNA damage response pathways like non-homologous end-joining (NHEJ) and homologous recombination (HR). There is evidence that tumors sometimes lack of efficient HR and therefore struggle with irradiation more than healthy tissue would do [23]. We investigated HR-efficiency by staining for RAD51 foci, as RAD51 is a main protein and essential for the HR pathway (Fig. 1F). Foci were counted after treatment with DNA-PK inhibitor CC-115 to force the cells to the usage of HR. BEAS-2B cells increased the amount of RAD51 foci after blockage of NHEJ, which leads to the assumption of HR-proficiency. In contrast, malignant A549 cells decreased the amount of RAD51 foci and were therefore defined as HR-deficient [19].

G2-block is detectable after treatment with crizotinib

Since it is known that different cell cycle phases show varying sensitivity to irradiation [24], we used a DNA staining approach to investigate the interaction of irradiation with kinase inhibitors on this cellular level (Fig. 2). Cells were stained with Hoechst dye and cells in G0/G1 as well as cells in G2/M phase were counted using histograms (Fig. 2A,B). Tumor cells A549 showed higher amounts of cells in G0/G1 phase in general. Treatment of cells with alectinib showed no influence neither of irradiation nor of kinase inhibitor or a combination of both (Fig. 2C). Noticeably, only crizotinib treatment led to an increase of the more radiosensitive G2/M phase in both cell lines, A549 (2 Gy: 11 % vs. 1 µM + 2 Gy: 51 %, 2 Gy: 11 % vs. 5 µM + 2 Gy: 61 %, 2 Gy: 11 % vs. 10 µM + 2 Gy: 37 %; p = 0.014) and

BEAS-2B (2 Gy: 24 % vs. 1 μM + 2 Gy: 46 %, 2 Gy: 24 % vs. 10 μM + 2 Gy: 45 %; p = 0.014) (Fig. 2D).

Migration is slightly influenced by ALK/ROS1 kinase inhibitors in both ALK/ROS1-wildtype cell lines

In the preclinical phase it is important to evaluate the toxicological potential of especially combination treatment schemes in different ways. Therefore, we used a scratch assays to investigate whether the addition of KIs to IR are able to influence the migratory potential of the cells (Fig. 3A and B) [25,26]. Area under the curve (AUC) was calculated for the curves of scratch closing over 48 h (Fig. S2), with a maximum value of 2 (no migration) and half-maximum of 1 (meaning an average half closing over 48 h). In general, both cell lines showed a similar migration behavior. At the physiological relevant concentrations of 0.1 μM and 1 μM KI migration was almost not influence while adding KI to radiotherapy, except the combination treatment in A549 which up-regulated the migration behavior significantly (2 Gy vs. 0.1 μM + 2 Gy: p = 0.029; 2 Gy vs. 1 μM + 2 Gy: p = 0.029). Over all, cells were less affected at concentrations of 0.1 and 1 μM but inhibited strongly when higher concentrations were used (Fig. 3C and D). Irradiation solely did not influence the migratory potential in a significant manner.

Discussion

There is evidence that simultaneously treatment with kinase inhibitors and radiotherapy could lead to unexpected and sometimes severe side effects [7], but sufficient data are still lacking for most KIs. To investigate whether a combinatory therapy of ALK/ROS1 kinase inhibitors crizotinib (first-generation) or alectinib (second-generation) with ionizing radiation could influence the effect of radiotherapy especially in normal tissue (ALK/ROS1 wildtype), we measured cell death and colony formation, as well as changes in the cell cycle and influence on the migratory behavior. Since normal, healthy tissue is always involved during radiotherapy and severe adverse effects like interstitial pneumonitis occurs frequently [27], we focused our study on the cell lines A549 and BEAS-2B, which are not harboring the KI-specific ALK/ROS1 mutations, representing normal lung tissue. Both epithelial cell lines are commonly utilized for investigation of radiosensitization events in lung tissue. Enhanced serum concretions of TGF- β are known to stand as risk factor of radio pneumonitis and Liu and colleagues demonstrated that A549 is able to increase the concentration of TGF-β after irradiation [28]. Additionally, TGF-b is a known inducer of epithelial-mesenchymal-transition (EMT) in A549, a relevant mechanism of development of RP [29]. Furthermore, the group of Heinzerling demonstrated recently less influence of simultaneously IR and ALKi treatment in two lung cancer cell lines, with no distinct radiosensitizing effect of ALKi in EML4-ALK mutated cells [30]. Live-cell imaging was used for a time-resolved detection of mitochondrial activity, apoptosis and necrosis. Time-resolved data gives deeper insights of cellular processes like mitochondrial activity, apoptosis and necrosis right after treatment. In general, treatment with both inhibitors concomitant to IR did mostly not lead to enhancement of toxicity in BEAS-2B and A549 (ALK/ROS1 wt). Just crizotinib seems to trigger a stronger apoptotic response in BEAS-2B, when compared to A549 + crizotinib. Here we might see an influence of the malignant and non-malignant origin of the two cell lines. According to the hallmarks of cancer, it is likely that tumor cells e.g. A549 harboring blocked or inadequate apoptosis signal pathways [31].

Analysis of toxicity showed no difference between the two ALK/ROS1-wt cell lines BEAS-2B and A549, but a response in a kinase inhibitor-dependent manner at concentrations of 5 and 10 μM ALKi respectively. Further analysis of e.g. colony forming ability were performed using inhibitor concentrations adapted to serum concentrations of the ALEX III trial, which let to approval of alectinib [32]. Additional irradiation did not lead to an increase of cell death. This might be of interest regarding the risk for radiation pneumonitis, as one of the most frequent adverse effects in the treatment of NSCLC. Since RP is based on an acute inflammation and inflammation could be trigged by cell death the immunogenic potential of combining IR with e.g. alectinib should be discussed. Our findings support the idea that concomitant IR + ALKi therapy does not lead to a significant increase of cell death at concentrations equal to serum concentrations, which might not lead to a relevant immunogenic trigger for the immune system. Cells responded stronger to first-generation KI crizotinib, due to a smaller specificity and possible off-target effects based on the additional effect on different kinases like c-Met and RON [33]. Interestingly, alectinib led to stronger decrease of number of colonies in our colony forming assay. We assumed that senescence is a primary way of action of alectinib compared to cell death. No data has been published yet to senescence-inducing ability of alectinib. Based on our hypothesis we want to emphasize that, in all cases IR led to enhancement of our tested treatment schemes in an additive manner, but not synergistically which could serve as an improvement of the cancer patient therapy avoiding additional side effects which are e.g. published for BRaf kinase inhibitor vemurafenib [6] or KI used for non-small cell lung cancer (NSCLC) [34]. Since vemurafenib showed less specificity compared to its second-generation BRafi (e.g. dabrafenib), pausing vemurafenib during RT is commonly recommended based on the increased risk of adverse effects. Off-target effects are explained by binding to related proteins like CRaf or wildtype BRaf affecting healthy tissue [6]. Such unwanted effects may not be suggested for alectinib because of its already published high binding specificity [9]. Furthermore, the current standard of care in lung cancer is a combination of RT with chemotherapy harboring a risk of side effects in up to 20 % of all patients, based on strong synergistic interactions of IR + CT [9,35]. Regarding the clinical safety of concomitant IR with ALK-inhibitors, this combination lacks such synergistic interactions. Interestingly, A549 seems to have an inefficient way of DNA double strand break repair (homologous recombination). We assumed that this inefficiency could explain the stronger decrease of colony formation. In accordance with this, previous findings showed a correlation of strong effect of DNA-PK inhibitor on cells lacking RAD51 [22].

Regarding the non-mutated ALK and ROS1 genes in both cell lines, they behaved similar to the kinase inhibitors each. Interestingly, crizotinib blocks the cells in the G2-phase, which might be based on the binding affinity of crizotinib to c-Met. The protein c-Met is involved in several cellular processes like survival and proliferation including the cell cycle [36]. G2-blockage after crizotinib treatment was also shown by Zhou et al. and Shrestha and colleagues [37,38]. The G2-phase is known to be more sensitive to irradiation [24], but increased cell death must not be the only consequence of G2 blockage. G2 arrest may also lead to pronounced senescence, rather than cell death. Senescence is a time-related process. Therefore, we assume no measurement of increased cell death after 48 h of treatment. Nevertheless, the detected G2 block is clinically relevant as therapeutic target, since it is measured 48 h after treatment (KI w/o IR). In a clinical setting a daily fractionated irradiation scheme could lead to accumulation of dead cells and may hold as additional stimulus during IR. If crizotinib lead to a stable G2 arrest this would expand the therapeutic window beneficially. Alectinib did not influence the cell cycle of our tested cell lines, since the second-generation inhibitor is known for less off-target effects including lower toxicities [2]. In the ALEX III trial (NCT02075840), which led to approval of alectinib, grade 3-5 adverse effects were detected for both inhibitors (alectinib vs. crizotinib: 41 % vs. 50 %). We showed, that increasing ALK inhibitor concentration lead to increase of toxicity, but adding IR to the treatment scheme does not enhance the toxicity further. Concomitant IR + KI therapy with a possible dose reduction of ALK inhibitors might therefore lead to improved tolerance, while decrease adverse effects, and still obtain adequate local tumor control through irradiation. The G2 arrest, detected after crizotinib, might enlarge the therapeutic window by shifting the cells in a more radiosensitive cell cycle phase during therapy.

Alectinib and crizotinib are both approved in the metastatic lung cancer situation. Therefore, influence on migration behavior is of important interest. Additionally, migration behavior can lead to evaluation of the toxicological potential. Our scratch assay data suggests that alectinib inhibits migration at physiological relevant concentrations of 1 µM KI (EMA – ALECENSA: Assessment report; Procedure No. EMEA/H/C/004164/0000). In general, both KI need high concentrations to decrease migration. Most importantly, concomitant KI + IR therapy showed no synergisms in our ALK/ROS1 wildtype cell lines.

Conclusions

In the presented study, the influence of simultaneously kinase inhibitor and irradiation therapy was investigated, on non-mutated ALK/ROS1 wt. cell lines, representing normal lung tissue. We showed the stronger influence of crizotinib on classical cell death pathways, whereas cells treated with alectinib responded stronger regarding colony formation, assumed to be influenced by senescence. Possibly, the G2-Block after crizotinib treatment is responsible for the increased cell death and the wider range of KI targets compared to alectinib. Surveillance over time showed stronger apoptotic response of BEAS after crizotinib compared to A549. In general, the live-cell data showed almost no difference between the treatment schemes especially IR vs. KI + IR and therefore supported our findings of cellular toxicity of the cell death and colony forming analysis. Both tested ALK and ROS1 wildtype cell lines (healthy and malignant) behaved quite similar and concomitant targeted therapy and radiotherapy lead to additive enhancement of cellular toxicity. However, both KIs lacked synergistic reinforcement, which could lead to an increase in the incidence and severity of side effects on normal tissues. Further investigation, also regarding new third-generation KI like lorlatinib, should be considered for the future [39]. In general, a combination of both kinase inhibitors seems to be well tolerated and does not contribute to increased toxicity in normal tissue.

Declaration of Competing Interest

M.H. reports collaborations outside this project with Merck Serono (advisory role, speakers' bureau, honoraria, travel expenses, research funding); MSD (advisory role, speakers' bureau, honoraria, travel expenses, research funding); AstraZeneca (research funding); Novartis (research funding); BMS (advisory role, honoraria, speakers' bureau); Teva (travel expenses). The other authors declare no conflict of interest.

CRediT authorship contribution statement

Tina Jost: Conceptualization, Methodology, Software, Validation, Formal analysis, Investigation, Data curation, Writing – original draft, Visualization, Supervision. **Ann-Kristin Schultz:** Formal analysis, Investigation. **Benjamin Frey:** Validation, Writing – review & editing. **Jennifer Vu:** Formal analysis, Investigation, Writing – original draft, Visualization. **Rainer Fietkau:** Resources. **Luitpold V. Distel:** Conceptualization, Methodology, Validation, Data curation, Writing – review & editing, Supervision, Project administration. **Markus Hecht:** Conceptualization, Validation, Writing – review & editing.

Funding

This research received no external funding.

Institutional review board statement

Not applicable.

Informed consent statement

Not applicable.

Acknowledgments

The authors would like to thank Doris Mehler and Lukas Kuhlmann for their excellent technical support of the study.

Supplementary materials

Supplementary material associated with this article can be found, in the online version, at doi:10.1016/j.neo.2022.100780.

References

[1] Arbour KC, Riely GJ. Systemic therapy for locally advanced and metastatic non-small cell lung cancer: a review. *JAMA* 2019;**322**(8):764–74.

[2] Peters S, et al. Alectinib versus crizotinib in untreated ALK-positive non-small-cell lung cancer. *N Engl J Med* 2017;**377**(9):829–38.

[3] Sause WT, et al. Fraction size in external beam radiation therapy in the treatment of melanoma. *Int J Radiat Oncol Biol Phys* 1991;**20**(3):429–32.

[4] Mazzola R, et al. Oligometastasis and local ablation in the era of systemic targeted and immunotherapy. *Radiat Oncol* 2020;**15**(1):92.

[5] Deutsch M, Parsons JA, Mercado R. Radiotherapy for intracranial metastases. *Cancer* 1974;**34**(5):1607–11.

[6] Hecht M, et al. Radiosensitization by BRAF inhibitor therapy-mechanism and frequency of toxicity in melanoma patients. *Ann Oncol* 2015;**26**(6):1238–44.

[7] Hecht M, et al. Clinical outcome of concomitant vs interrupted BRAF inhibitor therapy during radiotherapy in melanoma patients. *Br J Cancer* 2018;**118**(6):785–92.

[8] Anker CJ, et al. Avoiding severe toxicity from combined BRAF inhibitor and radiation treatment: consensus guidelines from the eastern cooperative oncology group (ECOG). *Int J Radiat Oncol Biol Phys* 2016;**95**(2):632–46.

[9] Jain V, Berman AT. Radiation pneumonitis: old problem, new tricks. *Cancers (Basel)* 2018;**10**(7).

[10] Soria JC, et al. Osimertinib in untreated EGFR-mutated advanced non-small-cell lung cancer. *N Engl J Med* 2018;**378**(2):113–25.

[11] Citrin DE, et al. Radiation-induced fibrosis: mechanisms and opportunities to mitigate. Report of an NCI workshop. *Radiat Res* 2017(1):1–20 p.188.

[12] Childs BG, Durik M, Baker DJ, van Deursen JM. Cellular senescence in aging and age-related disease: from mechanisms to therapy. *Nat Med* 2015;**21**(12):1424–35.

[13] Muñoz-Espín D, Serrano M. Cellular senescence: from physiology to pathology. *Nat Rev Mol Cell Biol* 2014;**15**(7):482–96.

[14] Larson-Casey JL, He C, Carter AB. Mitochondrial quality control in pulmonary fibrosis. *Redox Biol* 2020;**33**:101426.

[15] Cloonan SM, Choi AM. Mitochondria in lung disease. *J Clin Invest* 2016;**126**(3):809–20.

[16] Hofmann A, et al. Increase in non-professional phagocytosis during the progression of cell cycle. *PLoS One* 2021;**16**(2):e0246402.

[17] Reddel RR, et al. Transformation of human bronchial epithelial cells by infection with SV40 or adenovirus-12 SV40 hybrid virus, or transfection via strontium phosphate coprecipitation with a plasmid containing SV40 early region genes. *Cancer Res* 1988;**48**(7):1904–9.

[18] Cini N, et al. Modulation of radiation-induced oral mucositis (mouse) by dermatan sulfate: effects on differentiation processes. *Strahlenther Onkol* 2020;**196**(1):85–94.

[19] Mukhopadhyay A, et al. Development of a functional assay for homologous recombination status in primary cultures of epithelial ovarian tumor and correlation with sensitivity to poly(ADP-ribose) polymerase inhibitors. *Clin Cancer Res* 2010;**16**(8):2344–51.

[20] Dobler C, et al. Senescence induction by combined ionizing radiation and DNA damage response inhibitors in head and neck squamous cell carcinoma cells. *Cells* 2020;**9**(9).

[21] Faulhaber EM, et al. Kinase inhibitors of DNA-PK, ATM and ATR in combination with ionizing radiation can increase tumor cell death in HNSCC cells while sparing normal tissue cells. *Genes (Basel)* 2021;**12**(6).

[22] Burkel F, et al. Dual mTOR/DNA-PK inhibitor CC-115 induces cell death in melanoma cells and has radiosensitizing potential. *Int J Mol Sci* 2020;**21**(23).

[23] 18 Srivastava M, Raghavan SC. DNA double-strand break repair inhibitors as cancer therapeutics. *Chem Biol* 2015;**22**(1):17–29.

[24] Sinclair WK. Cyclic x-ray responses in mammalian cells *in vitro*. *Radiat Res* 1968;**33**(3):620–43.

[25] Timm DM, et al. A high-throughput three-dimensional cell migration assay for toxicity screening with mobile device-based macroscopic image analysis. *Sci Rep* 2013;**3**:3000.

[26] Lee NH, et al. SERPINB2 is a novel indicator of stem cell toxicity. *Cell Death Dis* 2018;**9**(7):724.

[27] Li F, et al. Risk factors for radiation pneumonitis in lung cancer patients with subclinical interstitial lung disease after thoracic radiation therapy. *Radiat Oncol* 2021;**16**(1):70.

[28] Liu W, Huang YJ, Liu C, et al. Inhibition of TBK1 attenuates radiation-induced epithelial–mesenchymal transition of A549 human lung cancer cells via activation of GSK-3β and repression of ZEB1. *Lab Invest* 2014:362–70.

[29] Xiong S, Pan X, Xu L, et al. Regulatory T cells promote β-catenin-mediated epithelium-to-mesenchyme transition during radiation-induced pulmonary fibrosis. *Int J Radiat Oncol Biol Phys* 2015;**93**(2):425–35.

[30] Fleschutz K, et al. ALK inhibitors do not increase sensitivity to radiation in EML4-ALK non-small cell lung cancer. *Anticancer Res* 2020;**40**(9):4937–46 Hanahan, D. and R.A. Weinberg, Hallmarks of cancer: the next generation. Cell, 2011. 144(5): p. 646-74.

[31] Zhou Y, et al. Off-target effects of c-MET inhibitors on thyroid cancer cells. *Mol Cancer Ther* 2014;**13**(1):134–43.

[32] Peters S, Camidge DR, Shaw AT, et al. Alectinib versus crizotinib in untreated ALK-positive non-small-cell lung cancer. *N Engl J Med* 2017;**377**(9):829–38.

[33] Borghetti P, et al. Radiotherapy and tyrosine kinase inhibitors in stage IV non-small cell lung cancer: real-life experience. *In Vivo* 2018;**32**(1):159–64.

[34] Peters S, et al. Alectinib versus crizotinib in untreated ALK-positive non-small-cell lung cancer. *N Engl J Med* 2017;**377**(9):829–38.

[35] Nagasawa S, et al. Why concurrent CDDP and radiotherapy has synergistic antitumor effects: a review of *in vitro* experimental and clinical-based studies. *Int J Mol Sci* 2021;**22**(6).

[36] Wood GE, et al. The role of MET in chemotherapy resistance. *Oncogene* 2021;**40**(11):1927–41.

[37] Zhou Y, et al. Off-target effects of c-MET inhibitors on thyroid cancer cells. *Mol Cancer Ther* 2014;**13**(1):134–43.

[38] Shrestha N, et al. Mechanisms of suppression of cell growth by dual inhibition of ALK and MEK in ALK-positive non-small cell lung cancer. *Sci Rep* 2019;**9**(1):18842.

[39] Richter J, Dunst J. [Lorlatinib: a promising drug in the future treatment of advanced ALK-positive non-small-cell lung cancer]. *Strahlenther Onkol* 2021;**197**(7):657–60.